Macromolecules

ARTICLE

pubs.acs.org/Macromolecules

Segmental Dynamics of Dilute Poly(ethylene oxide) in Low and High Molecular Weight Glass-Formers

Junshu Zhao and M. D. Ediger*

Department of Chemistry, University of Wisconsin—Madison, Madison, Wisconsin 53706, United States

ABSTRACT: Deuterium NMR at Larmor frequencies of 15.6 and 76.7 MHz was used to study the segmental dynamics of dilute perdeuteriopoly(ethylene oxide) (d_4PEO) in equilibrium miscible mixtures with four low molecular weight glass-formers: indomethacin, sucrose benzoate, *o*-terphenyl, and toluene. Results are compared with literature data for dilute PEO in two polymer hosts: poly(methyl methacrylate) (PMMA) and poly(vinyl acetate) (PVAc). The segmental dynamics of PEO are found to strongly correlate with the dynamics of both high and low molecular weight hosts. For dilute PEO in mixtures with PMMA, PVAc, and sucrose benzoate, the Lodge−McLeish model with a ϕ_{self} (self-concentration) of 0.35 gives a good fit to the dynamics of dilute PEO, similar to previously reported dilute polyisoprene blends and dilute polystyrene blends. A smaller ϕ_{self} is obtained for dilute PEO in indomethacin, consistent with the presence of a hydrogen-bonding effect. For PEO in *o*-terphenyl and toluene, the implementation of the Lodge−McLeish model utilized here fails to give quantitative fits for the dynamics of the dilute PEO chains; this result is obtained because the full temperature-dependent host dynamics are not utilized in the fitting procedure.

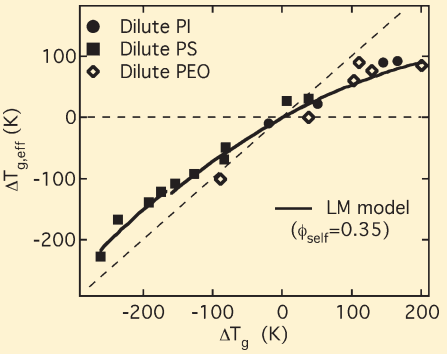

INTRODUCTION

Poly(ethylene oxide) (PEO) has a broad range of applications. It is used as the hydrophilic component in nonionic surfactants and as a controlled release agent for drug delivery, and it is extensively studied for use in lithium−polymer batteries as the electrolyte. For polymer systems, many important material properties including the glass transition temperature T_g, the mechanical response, and the transport behavior of small molecules are strongly correlated with the dynamics of the polymer components. For example, it has been shown both by experiment[1] and molecular dynamics simulation[2] that the conductivities of PEO−salt mixtures are strongly coupled with the segmental dynamics of PEO. On the other hand, the segmental dynamics of the PEO chains are also modified by the presence of both high and low molecular weight blending partners. An enhanced understanding of PEO segmental dynamics in mixtures would allow better predictions of the properties of materials that contain PEO.

The segmental dynamics of PEO in miscible polymer blends have been carefully investigated.[3−14] Lutz et al.[3] reported that, in PEO/poly(methyl methacrylate) (PMMA) blends, the segmental dynamics of PEO was up to 12 orders of magnitude faster than those of PMMA. They reported that the Lodge−McLeish model,[15] which can successfully fit the component segmental dynamics in many polymer blends, failed to fit the segmental dynamics of PEO in blends with PMMA. Genix et al.[7] reported significant broadening of the PEO segmental relaxation time distribution in this blend below the T_g of the PMMA component. They proposed that the broadening results from the vitrification of the PMMA component and that this increases the mobility of PEO in the blend. Zhao et al.[14] studied the segmental dynamics of PEO in blends with poly(vinyl acetate) (PVAc).[16−18] While PEO segmental dynamics can be faster than that of PVAc by up to 10 orders of magnitude, this occurs while both components are in equilibrium, and the Lodge−McLeish model gives very good fit to the data. This suggests that the failure of the Lodge−McLeish approach to describe the dynamics of PEO in PMMA is due to the vitrification of the PMMA component. In equilibrium mixtures, the available data indicate that the segmental dynamics of PEO in miscible polymer blends is reasonably well understood.

Given the importance of mixtures of PEO and low molecular weight compounds in many applications, it is useful to attempt to extend our understanding of segmental dynamics in miscible polymer blends containing PEO to a broader class of mixtures. The conceptual basis of the Lodge−McLeish model, self-concentration due to chain connectivity, should be equally valid for a polymer surrounded by a low molecular weight host as it is for high molecular weight host.[19,20] Extending the study of PEO dynamics in miscible polymer blends to polymer−small molecule mixtures might be useful in two ways. First, it tests the range of validity and transferability of the self-concentration concept. Second, since there is a much wider variety of miscible polymer/small molecule mixtures than miscible polymer blends, considering low molecular weight compounds allows us to broaden the spectrum of blending partners. Testing the Lodge−McLeish model in these systems may reveal imperfections in the model that are not clearly observed in polymer blends and suggest ways to modify and improve the model.

Received: August 18, 2011
Revised: October 8, 2011
Published: October 21, 2011

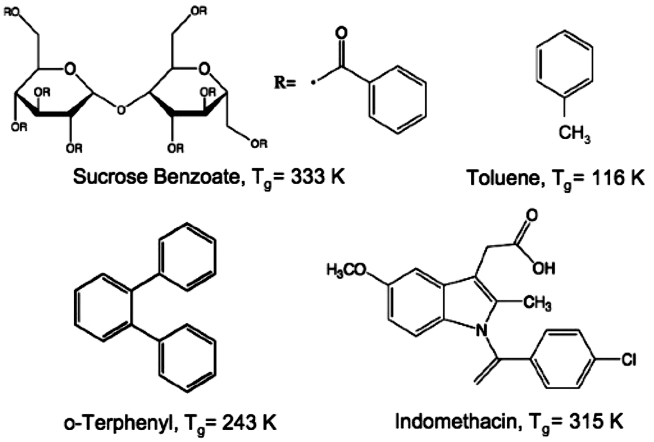

Figure 1. Low molecular weight hosts used in this study. Glass transition temperatures are indicated.

Here we report ^{2}H NMR measurements of the segmental dynamics of perdeuteriopoly(ethylene oxide) (d_4PEO) in miscible mixtures with four low molecular weight glass-formers: toluene, sucrose benzoate, *o*-terphenyl, and indomethacin (a typical amorphous pharmaceutical[21−25]). The T_g values of the hosts cover a broad temperature range (116−333 K). To simplify the problem, and in particular to eliminate the effect of intermolecular concentration fluctuations,[26] we studied each mixture in the dilute regime (1% d_4PEO). For each system, we performed ^{2}H NMR T_1 measurements at two different magnetic fields. All measurements were performed in the equilibrium state above the T_g of both components. Segmental correlation times for PEO were extracted using a modified Kohlrausch−Williams−Watts (mKWW) correlation function. Results are compared with those for PEO/PMMA and PEO/PVAc blends and with results for other miscible blends.

We find that the segmental dynamics of PEO are qualitatively consistent with the prediction of the Lodge−McLeish model in that slower segmental dynamics are generally observed in mixtures with higher T_g hosts. However, our implementation of the Lodge−McLeish model was not able to provide a good description of the data for all the systems studied. For PEO in sucrose benzoate, a self-concentration (ϕ_{self}) of 0.28 gives a good description of the segmental dynamics of dilute PEO in the mixture; this is close to the previously reported value for equilibrium blends of PEO in PMMA and PEO in PVAc.[14] For PEO in indomethacin, the Lodge−McLeish fit results in a smaller ϕ_{self} value of 0.12, indicating that indomethacin exerts a greater influence on the dynamics of PEO than do the other blending partners. We interpret this observation to be the result of intermolecular hydrogen bonding between PEO and indomethacin. For PEO in *o*-terphenyl, the Lodge−McLeish fit could not capture the temperature dependence of the segmental dynamics of dilute PEO. For PEO in toluene, the fit yields an unphysical negative ϕ_{self} value. The apparent failure of the model for these last two systems likely occurs because of the simplified manner in which the dynamics of the host are represented in the fitting process.

MATERIALS AND METHODS

Materials. Perdeuteriopoly(ethylene oxide) (d_4PEO) with protio termination was purchased from Polymer Source (P3887- dPEO2MeO). The d_4PEO has M_n = 1800 g/mol and M_w/M_n = 1.08. Indomethacin was purchased from Sigma (I7378), sucrose benzoate was purchased from Aldrich (458333), and *o*-terphenyl was purchased from Aldrich (T280-0). The toluene used here is ACS reagent grade. The structures of the low molecular weight hosts are shown in Figure 1.

Mixture Preparation. Samples of dilute d_4PEO in *o*-terphenyl and toluene were prepared by directly mixing the desired amount of the components in glass vials. Samples were stirred overnight and transferred into NMR tubes, which were then sealed under vacuum. Sucrose benzoate and indomethacin are solids at room temperature and dilute d_4PEO solutions in these hosts were made by a melt mixing method described as follows. The desired amount of d_4PEO and the host were combined in a glass vial. The mixture was then heated to ∼170 °C, a temperature at which both hosts are low-viscosity liquids. Samples were stirred under nitrogen at this temperature for about 10 min and then quickly cooled to room temperature. The resulting solid mixture was then broken into small pieces and transferred into a NMR tube. The tube was then held in a vacuum oven for 24 h at room temperature and then briefly heated in the vacuum oven to 170 °C. This treatment sufficed to remove moisture from the sample and to induce flow into the bottom of the NMR tube. The tube was then sealed under vacuum before measurements.

T_g and Miscibility. The glass transition temperatures (T_g) for sucrose benzoate, indomethacin, *o*-terphenyl, and toluene are 333, 315, 243, and 116 K, respectively. The T_g of the d_4PEO used in this work was not directly measured due to rapid crystallization of pure d_4PEO. A previous study showed that high molecular weight PEO (M_n ∼ 150 000 g/mol) has a T_g of 211 K.[16] We found that the NMR T_1 data for the low molecular weight PEO used in this work can be superposed with the data for 150 000 g/mol PEO[3] after a 5 K shift to higher temperatures; hence, we estimate the T_g of the low molecular weight PEO as 206 K. Since the hosts used in this study have T_g values that are quite different from that of PEO (by 40−130 K), any small error associated with this T_g estimate does not significantly affect the analysis of our data.

We have good evidence that all these systems are miscible in the temperature regime of this study. Toluene is a known solvent of PEO.[7,27] A melting point depression for indomethacin was observed for dilute PEO/indomethacin mixtures, suggesting miscibility of this system. The low concentration and the low molecular weight of the d_4PEO used here facilitate miscibility. NMR tests done on all four systems further support miscibility (see below).

NMR Measurements. Spin−lattice relaxation times T_1 were measured using ^{2}H NMR and the standard inversion recovery ($\pi-\tau-\pi/2$) pulse sequence. ^{2}H NMR measurements were performed at two frequencies using a Varian Inova-500 NMR spectrometer (76.7 MHz) and a Bruker DMX NMR spectrometer (15.6 MHz). Temperature was controlled to ±0.5 K and calibrated to an uncertainty of ±2 K using a methanol thermometer at low temperatures, an ethylene glycol thermometer at ambient and moderately elevated temperatures, and melting point standards at high temperatures. Data were processed with line broadening equal to one-tenth the line width of the resonance peak, and T_1 was obtained from the magnetization relaxation by fitting with three parameters. At higher temperature, intensities and peak areas were separately employed for the fit and yielded T_1 values that agreed to within the experimental error (7%) of our measurements. At lower temperatures the resonance peaks are broader and peak areas better represent the average magnetization of the PEO segments; hence, T_1 values were extracted from the area analysis.

For samples of 1% d_4PEO in sucrose benzoate and *o*-terphenyl, after exposure to high temperatures, T_1 was reacquired at lower temperatures as a test of sample degradation; the T_1 measurements after exposure to high temperatures agreed with earlier measurements to within experimental error. Since indomethacin is prone to crystallization, NMR measurements on samples containing indomethacin were performed starting at the highest temperature, and a different test for sample degradation was used; DSC measurements on the sample before and after NMR measurements were consistent and provided no evidence for

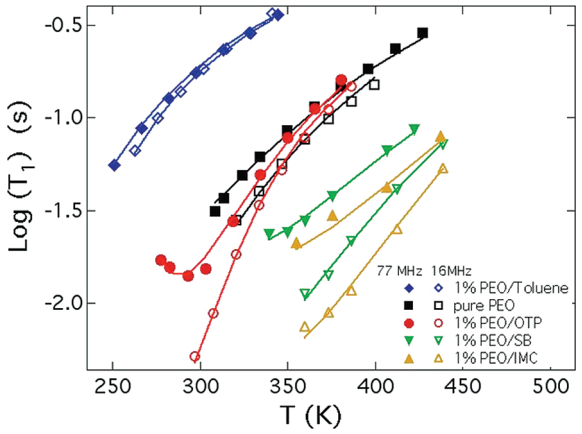

Figure 2. NMR T_1 data and fits for dilute d_4PEO in four low molecular weight glass-forming hosts as a function of temperature. Also shown are results for neat d_4PEO. For each system, solid symbols represent T_1 data for 77 MHz and open symbols represent data for 16 MHz. Solid lines are obtained by simultaneously fitting the data for each system at both fields using eqs 1−5.

crystallization or degradation. Sucrose benzoate, *o*-terphenyl, and toluene are good glass-formers, and crystallization did not occur in our measurements. Because of the low concentration of PEO, its melting point is significantly depressed and PEO crystallization was not observed in the temperature range for which we report NMR measurements.

NMR Data Interpretation. Spin−lattice relaxation times (T_1) for d_4-PEO in the pure state and in dilute mixtures are reported here. T_1 is the characteristic time for an inverted magnetization to relax back to equilibrium. For deuterium nuclei, spin−lattice relaxation is dominated by electric quadrupole coupling and has the following relationship to the reorientation of a C−D bond:[28,29]

$$\frac{1}{T_1} = \frac{3}{10}\pi^2\left(\frac{e^2qQ}{h}\right)^2 [J(\omega_D) + 4J(2\omega_D)] \quad (1)$$

Here $\omega_D/2\pi$ is the Larmor frequency and e^2qQ/h is the quadrupole coupling constant.[5] $J(\omega)$ is the spectral density function and quantifies the power available at frequency ω to relax the ^{2}H spins. $J(\omega)$ is the Fourier transform of the orientation autocorrelation function $G(t)$:

$$J(\omega) = \frac{1}{2}\int_{-\infty}^{\infty} G(t)e^{-i\omega t}\,dt \quad (2)$$

$G(t)$ describes randomization of the orientation of C−D vectors as a function of time and has the following form:

$$G(t) = \frac{3}{2}\langle\cos^2\theta(t)\rangle - \frac{1}{2} \quad (3)$$

Here $\theta(t)$ is the angle of a C−D bond relative to its orientation at time $t = 0$. If no reorientation has occurred, $G(t)$ will have a value of unity, whereas if the C−D vector has realized all orientations on the unit sphere with equal probability, the function will have decayed to zero. In evaluation of eq 2, $G(-t) = G(t)$ is utilized.

The decay of $G(t)$ is caused by three motions: librational motion, segmental motion, and larger length scale motions including terminal relaxation. For our experiments, the contribution of the larger length scale motions is neglected due to the insignificant influence on C−D bond reorientation.[29,30] Based on previous studies,[30−34] the modified Kohlrausch−Williams−Watts (mKWW) function gives an excellent representation of the C−D bond orientation autocorrelation function:

$$G(t) = a_{lib}e^{-t/\tau_{lib}} + (1 - a_{lib})e^{-(t/\tau_{seg})^{\beta}} \quad (4)$$

Table 1. Fit Parameters for Neat d_4PEO and 1% d_4PEO in Four Glass-Forming Hosts[a]

host	PEO	OTP	IMC	SB	toluene
τ_∞ (ps)	0.02	0.19	0.01	0.01	0.09
T_0 (K)	180	240	260	250	102
β	0.27	0.33	0.25	0.23	0.35
B (K)	354	178	354	354	354

[a] For these fits, B and a_{lib} were constrained to be 354 K and 0.1, respectively, except for dilute PEO in OTP where only a_{lib} was constrained to 0.1.

Here a_{lib} and τ_{lib} characterize the amplitude and relaxation time for the librational motion. β describes the distribution of the segmental relaxation processes associated with τ_{seg}. We assume that τ_{seg} has Vogel−Tammann−Fulcher (VTF) temperature dependence:

$$\log\left(\frac{\tau_{seg}}{\tau_\infty}\right) = \frac{B}{T - T_0} \quad (5)$$

Here τ_∞, B, and T_0 are constants for a given component in a particular blend. The correlation time for segmental dynamics $\tau_{seg,c}$ is the time integral of the segmental portion of the correlation function:

$$\tau_{seg,c} = \frac{\tau_{seg}}{\beta}\Gamma\left(\frac{1}{\beta}\right) \quad (6)$$

RESULTS

NMR T_1 Data. Figure 2 shows the measured ^{2}H T_1 values for pure d_4PEO and for 1% d_4PEO in the four low molecular weight glass-forming hosts. Data were acquired at ^{2}H Larmor frequencies of 15.6 and 76.7 MHz. The maximum temperature for each sample was set to avoid degradation or, for the case of toluene, vaporization. For 1% d_4PEO in *o*-terphenyl (OTP), indomethacin (IMC), and sucrose benzoate (SB), the minimum temperature is determined by the temperature at which the fwhm line width was around 10 000 Hz; when the line is wider, the PEO component can no longer be considered as a liquid when analyzing T_1 measurements. For neat d_4PEO and for 1% d_4PEO in toluene, the minimum temperature is determined by crystallization. As the temperature is lowered, a minimum in T_1 is expected; only for OTP at 76.7 MHz does the accessed temperature range include the T_1 minimum. The error bars for the T_1 measurements are about the same size as the symbols.

Fitting of the deuterium T_1 data for pure d_4PEO and dilute d_4PEO in the four glass-formers was performed with eqs 1−5. Data for each system were fit simultaneously for both fields. In this fitting procedure there are five unknown parameters: a_{lib}, τ_∞, β, B, and T_0. For pure PEO and dilute PEO in sucrose benzoate, indomethacin, and toluene, B and T_0 are highly correlated with each other because of the relatively small range of correlation times sampled in these measurements. To be consistent with the fits for pure PEO in the study of PEO/PMMA[3] and PEO/PVAc,[14] B was constrained to be 354 K for these systems. In addition, we have constrained the a_{lib} to a value of 0.1, also to be consistent with the study on PEO/PMMA and PEO/PVAc. For dilute PEO in *o*-terphenyl, however, constraining B to be 354 K failed to yield an adequate fit that captures the low temperature T_1 trend; for this system, the only fitting constraint applied was $a_{lib} = 0.1$. The fitted T_1 values for each system are shown in Figure 2 as solid curves. The fits give a good representation of the

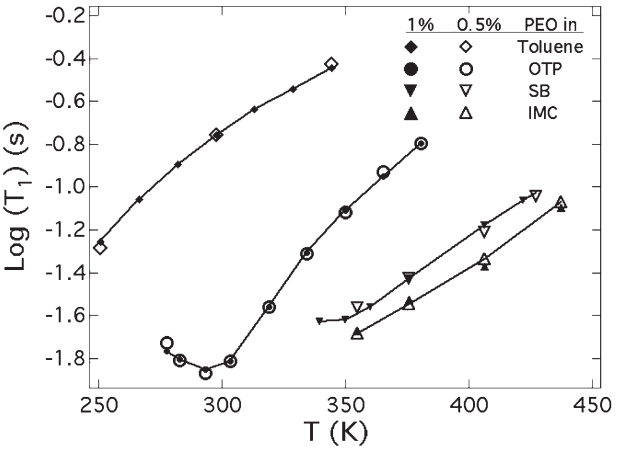

Figure 3. Comparison of NMR T_1 data for 0.5% and 1% d_4PEO in four low molecular weight glass-forming hosts at 77 MHz. Solid symbols represent data for 1% PEO blends, and open symbols represent data for 0.5% PEO blends. Solid lines are used to guide the eye.

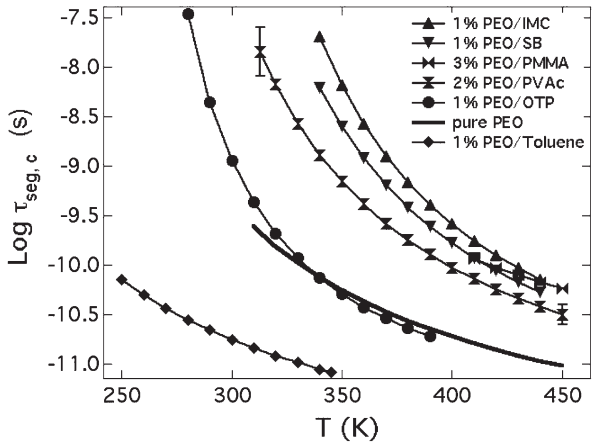

Figure 4. Segmental correlation times of pure d_4PEO and dilute d_4PEO in four low molecular weight glass-forming hosts. Also included are results for dilute d_4PEO in PMMA (ref 3) and in PVAc (ref 14). In all cases, the correlation times are calculated from the NMR T_1 data as described in the text. Errors associated with the calculated segmental correlation times are similar for all systems, and representative error bars are shown on the 2% PEO/PVAc curve.

data. Compared to unconstrained fits, adding the constraints described above did not significantly affect the fitting quality and did not have a significant impact on the $\tau_{seg,c}$ values that we report below. The parameters for the fits shown in Figure 2 are given in Table 1. Because of the broad distribution of relaxation times and the limited temperature range, an array of fitting parameters provided comparable fits. When adjusted together, a wide range of B (over 100 K) and T_0 (over 100 K) can fit the data. Consequently, correlation times calculated from the parameters in Table 1 can only be considered accurate within the experimental temperature range.

Miscibility Check by NMR. We performed NMR experiments to confirm the miscibility of the four systems studied here. Mixtures containing 0.5% of d_4PEO in each host were prepared. T_1 measurements at 76.7 MHz were carried out on each 0.5% mixture, and the data are compared with those of the corresponding 1% mixture in Figure 3. For all four systems, the data for

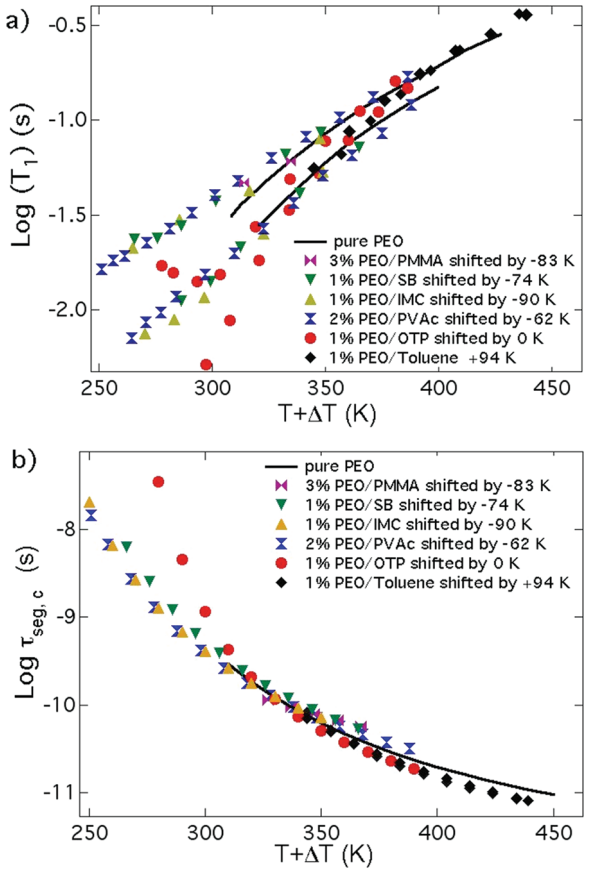

Figure 5. T_1 measurements (panel a) and calculated segmental correlation times (panel b) for dilute d_4PEO in different hosts, shifted to those of pure d_4PEO. In panel a, NMR data at 77 MHz (larger T_1 values) and 16 MHz (smaller T_1 values) are represented by the same symbols for a given system. The temperature shifts applied are indicated in the legends. Also included are data for dilute d_4PEO in PMMA (ref 3) and in PVAc (ref 14).

the two compositions agree very well. If phase separation had occurred in either or both of the 1% and 0.5% mixtures, a difference in the T_1 data would be expected. In addition, if phase separation occurs, different T_1 relaxation times are expected for different phases, in which case the decay of the inverted magnetization should be nonexponential. For all our data, excellent single-exponential decays were observed, further supporting the miscibility of the mixtures in the temperature range of our study.

Segmental Correlation Times. Figure 4 shows the segmental correlation times $\tau_{seg,c}$ of d_4PEO as pure polymer and as the dilute component in four low molecular weight glass-forming hosts. In addition to the systems studied here, data for dilute PEO in PMMA[3] and in PVAc[14] above their blend T_gs are also included. In Figure 4, we see that the segmental correlation times of d_4PEO in the low molecular weight hosts span the PEO correlation times in polymer hosts. At 350 K, segmental correlation times of PEO in the various hosts span 3 decades. It is worth noting that the segmental dynamics of PEO are slowest (by a small factor) in indomethacin, even though indomethacin has a lower T_g than both PMMA and sucrose benzoate. Also note that the dynamics of PEO in *o*-terphenyl intersect with those of pure PEO even though *o*-terphenyl has a T_g almost 40 K higher than that of PEO.

dx.doi.org/10.1021/ma201889b |*Macromolecules* 2011, 44, 9046–9053

The $\tau_{seg,c}$ values for dilute d_4PEO in the four low molecular weight glass-formers were calculated from eq 6 using the fit parameters shown in Table 1. For all the systems, an error bar of ±0.25 decades is associated with the segmental correlation times at the lowest temperatures; this error diminishes to ±0.1 decades at the highest temperatures. Representative error bars are shown on the curve for the 2% PEO/PVAc blend. Although the PEO samples used for the PMMA and PVAc studies have different molecular weights than the PEO used here, the segmental dynamics of the pure PEO samples are consistent to within 0.1 decade. This allows a direct comparison of the dilute PEO/PMMA and PEO/PVAc blends with the systems studied here.

Data Superposition. A model independent analysis of the effect of mixing on the segmental dynamics of PEO can be made by directly superposing the mixture T_1 data with the data for pure d_4PEO. A master superposition plot of d_4PEO T_1 values in all mixtures is given in Figure 5a. Only temperature shifts were employed. The resulting superposition is satisfactory for pure PEO and dilute PEO in PMMA, PVAc, sucrose benzoate, and indomethacin. This means that the segmental correlation times of PEO in these systems are roughly the same as those of pure PEO with a shift in temperature. Data for dilute PEO in toluene and especially in *o*-terphenyl, however, have different temperature dependences than the master curve. This indicates that the dynamic behavior of dilute PEO in these two systems is more complex than just a temperature shift from the dynamics of pure PEO. A similar shifting procedure was performed on the calculated segmental relaxation times for PEO in each host system as shown in Figure 5b; the same temperature shifts used in Figure 5a are applied. Satisfactory superposition was obtained except for dilute PEO in OTP, which again has a clear difference in the temperature dependence relative to the master curve. The consistency between the two superposition plots in Figure 5 provides additional support for the validity of the model that is used to fit the NMR data and extract the segmental correlation times.

DISCUSSION

Lodge−McLeish Description of PEO Segmental Dynamics in Different Hosts. In the Lodge−McLeish model,[15] the mobility of a given polymer segment is determined by the chemical composition of the region within one cubic Kuhn length (l_K) of the segment. This local concentration (ϕ_{eff}) is calculated from the bulk concentration (ϕ) and the self-concentration (ϕ_{self}) that results from the connectivity of the polymer chain:

$$\phi_{eff} = \phi_{self} + (1 - \phi_{self})\phi \quad (7)$$

Lodge and McLeish have estimated the self-concentration ϕ_{self} as

$$\phi_{self} = \frac{C_\infty M_0}{\kappa \rho N_{av} V} \quad (8)$$

where C_∞ is the characteristic ratio, M_0 is the repeat unit molar mass, κ is the number of backbone bonds per repeat unit, ρ is the density, N_{av} is Avogadro's number, and $V = l_K^3$.

In this model, polymer segments of a given type have an effective glass transition temperature that is different from the macroscopic blend T_g because the local composition (ϕ_{eff}) differs from the bulk composition (ϕ). This effective glass transition temperature is denoted as $T_g(\phi_{eff})$ and can be approximately

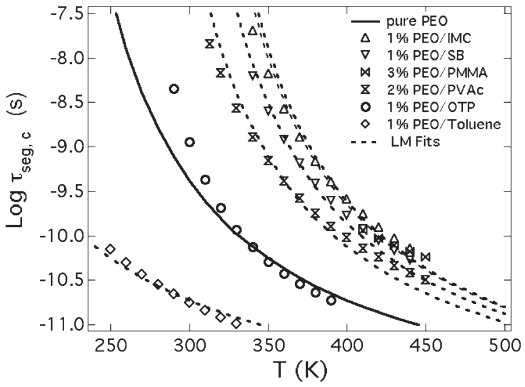

Figure 6. Fits of the Lodge−McLeish model to the segmental dynamics of dilute d_4PEO in various hosts. The solid curve represents pure PEO dynamics and is used as an input in the fitting procedure. From top to bottom, the dotted lines represent fits for dilute PEO in indomethacin, PMMA, sucrose benzoate, PVAc, and toluene, respectively. The corresponding ϕ_{self} values are 0.12, 0.37, 0.28, 0.30, and −0.24. For dilute PEO in OTP, the crossing of the segmental correlation times with those for pure PEO indicates a failure of an assumption of our fitting procedure, and thus no fit is shown. Points in the figure are calculated segmental relaxation times.

calculated from the Fox equation:

$$\frac{1}{T_g(\phi_{eff})} = \frac{\phi_{eff}}{T_{g,A}} + \frac{1 - \phi_{eff}}{T_{g,B}} \quad (9)$$

The original work of Lodge and McLeish concerns only the behavior in the vicinity of the glass transition temperature. In our implementation of their model, we add the assumption that segmental dynamics in the blend can be predicted by correlating changes in T_g with changes in the T_0 that appears in eq 5. For a given component

$$T_{0,i}(\phi) = T_{0,i} + [T_{g,i}(\phi) - T_{g,i}] \quad (10)$$

If this approach is valid, component dynamics in a mixture can be predicted by applying a temperature shift to the segmental correlation times of the pure homopolymer.

Figure 6 shows the segmental relaxation times for neat d_4PEO and for d_4PEO as a dilute component in different hosts, with the dotted lines showing the best fits to the Lodge−McLeish model, obtained by treating ϕ_{self} as a fitting parameter. For these fits, the VTF curve describing the pure PEO dynamics is needed as an input. Because of the crystallization of PEO, pure PEO dynamics cannot be measured at lower temperatures. The VTF parameters for PEO dynamics determined by fitting the data at higher temperatures were used to extrapolate the correlation times to lower temperatures. At the estimated T_g (206 K) of the pure PEO, the extrapolated segmental correlation time is 20 s, consistent with the commonly accepted range of 10−100 s; this supports the validity of the extrapolation used here.

The quality of the Lodge−McLeish fits in Figure 6 differs significantly among the host matrices. For most hosts (PMMA, PVAc, sucrose benzoate, and indomethacin), the fits shown in Figure 6 are reasonable given the error bars. However, in contrast to eq 8, which indicates that PEO dynamics in different systems can be described by a single ϕ_{self} value, the ϕ_{self} values determined from the fits are different among the four systems. For dilute PEO in PMMA, PVAc, and sucrose benzoate, values of ϕ_{self} near 0.3 were obtained. Although this value is larger than the value

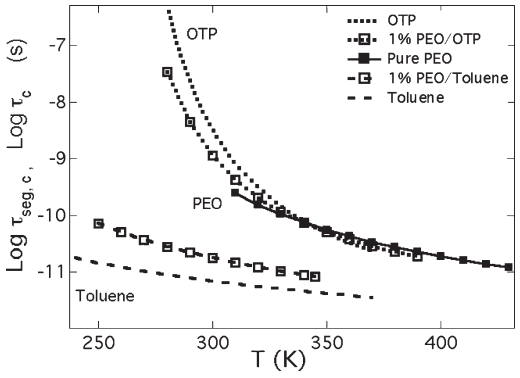

Figure 7. Structural relaxation times of pure *o*-terphenyl (OTP) and pure toluene along with segmental correlation times for neat PEO and dilute PEO in blends with *o*-terphenyl and toluene. The segmental correlation times shown in the figure were calculated from NMR data.

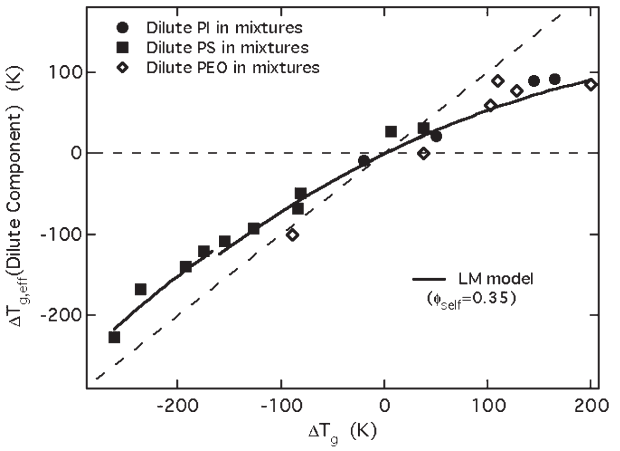

Figure 8. Dynamics of dilute polymers as a function of host T_g values. The figure is adapted from Figure 10 in ref 34. Solid symbols are for dilute PS blends, solutions, and diluted PI blends from the original figure. Open diamonds are data for PEO mixtures from this work and refs 3 and 14.

predicted by eq 8 (0.15), it is similar to the ϕ_{self} values obtained by fitting data for many other flexible polymers in miscible blends.[34−36] This suggests that the dynamics of PEO change in a typical manner upon mixing with these three hosts. A smaller value of ϕ_{self} (0.13) was obtained for dilute PEO in indomethacin, indicating that PEO dynamics in this mixture are affected by the (slower) host to a greater extent. This type of behavior has been previously observed for polymer blends with strong intermolecular hydrogen bonding.[37−39] For PEO in indomethacin, we speculate that hydrogen bonding between the PEO oxygen and the acidic proton of indomethacin is responsible for the smaller value of ϕ_{self}.

Our implementation of the Lodge−McLeish model cannot rationalize the dynamics of dilute PEO in *o*-terphenyl and toluene. *o*-Terphenyl has a T_g that is roughly 40 K higher than PEO, indicating slower dynamics than neat PEO at low temperatures. Hence, upon mixing, the dynamics of dilute PEO in *o*-terphenyl are expected to be slower than neat PEO dynamics. While this expectation is consistent with the lower temperature data in Figure 6, at higher temperatures PEO in *o*-terphenyl is slightly more mobile than is neat PEO. The segmental dynamics of dilute PEO in toluene is even more intriguing in that a negative ϕ_{self} (−0.24) was extracted from the fit. (For comparison, if a value of ϕ_{self} = 0.3 were used to describe the PEO/toluene data, the fit curve would be displaced 28 K to the right.) A negative ϕ_{self} not only violates the physical picture of the Lodge−McLeish model but also suggests that the segmental dynamics of PEO in toluene is even faster than the dynamics of neat toluene. It has been previously reported that dilute polystyrene in toluene can be described by a positive ϕ_{self} value, although the best-fit value is smaller than both the prediction of eq 8 and the value obtained with polymeric hosts.[34]

To understand the dynamics of dilute PEO in *o*-terphenyl and toluene, we plot in Figure 7 the rotational correlation times of neat toluene and neat *o*-terphenyl, along with the segmental correlation times of pure PEO and dilute PEO in these two solvents. The rotational correlation times of neat *o*-terphenyl were obtained by using the temperature dependence of the viscosity data in the range of interest[40] to extend the α relaxation time measured by dielectric relaxation at lower temperatures.[41] The rotational correlation times of neat toluene were obtained by using the temperature dependence of the viscosity data in the range of interest[42] to extend the rotational correlation times measured by NMR at low temperatures.[43] These procedures were validated against ^{2}H NMR measurements of rotational correlation times available over part of the temperature range shown.[44,45]

For each system shown in Figure 7, the dynamics of the dilute PEO component lies between the dynamics of pure PEO and the dynamics of the neat host. This behavior is qualitatively consistent with the self-concentration concept. The conflict between the conclusions drawn from Figure 6 and Figure 7 is a result of our implementation of the Lodge−McLeish model. According to eqs 7, 9, and 10, the dynamics of dilute PEO can be predicted at any temperature from the segmental dynamics of neat PEO, the value of ϕ_{self}, and the T_g of the host. This is a reasonable if the dynamics of the pure components increase with temperature at similar rates, so that the relationship between the dynamics of the two components at low temperatures is retained at high temperatures. For both neat *o*-terphenyl and neat toluene, dynamics speed up with increasing temperature much faster than those of neat PEO. The failure of our implementation of the Lodge−McLeish model likely occurs because the fundamental factor controlling the dynamics of PEO in mixtures is the local relaxation times of the blending partner instead of its T_g.

These results suggest that a more quantitative implementation of the self-concentration model should utilize the entire temperature dependence of the dynamics of the two pure components. There are two methods described in the literature that use such an approach for predicting dynamics in polymer blends. The first is a method proposed by Cangialosi et al.[46] that is based upon the Adam−Gibbs model of the glass transition.[47] Here the Adam−Gibbs parameters of the two pure components are averaged to predict component dynamics in the blend. However, this method requires supplementary calorimetry[46] or dynamics[48] data in order to extract the parameters for the pure components. The second method was proposed by Kamath et al.;[49] here the WLF parameters that describe the temperature dependences of the pure component dynamics were averaged to predict component dynamics in the blend. However, neither toluene nor *o*-terphenyl can be described by a single set of WLF (or VTF) parameters over the temperature range of interest, and thus this approach cannot be applied to our data in a straightforward

manner. While these two methods of implementing the Lodge−McLeish model have not yet been widely applied, they do provide ideas that may improve the predictive power of self-concentration models for systems in which the temperature dependences of the dynamics of the pure components are strongly mismatched.

Comparing Dynamics of Dilute PEO Mixtures with Other Dilute Polymer Systems. Figure 8 shows the $\Delta T_{g,eff}$ (the difference between $T_{g,eff}$ resulting from the Lodge−McLeish fit and the T_g of pure homopolymer) as a function of the T_g difference between the two pure components. The plot is modified from Figure 10 in ref 34. In addition to the data for dilute polyisoprene (PI) mixtures and dilute polystyrene (PS) mixtures from ref 34, we also plot the data for dilute PEO mixtures. If the segmental dynamics of a dilute chain were completely coupled to the dynamics of the host, the system would be represented by a point on the line of slope = 1 ($\phi_{self} = 0$). On the other hand, if the segmental dynamics of the dilute chain did not change upon blending, the system would be represented by a point on the line of slope = 0 ($\phi_{self} = 1$). The solid curves in Figure 8 are calculated from the Lodge−McLeish model by assuming a ϕ_{self} of 0.35. The six systems containing dilute PEO chains (data in Figures 4−6) are shown in Figure 8 as open diamonds.

Figure 8 shows that while ϕ_{self} for PEO in dilute mixtures cannot be predicted by eq 8, these systems fit reasonably well into the general pattern established by the PS mixtures and PI blends with a ϕ_{self} of 0.35. For dilute PEO in PMMA, PVAc, and sucrose benzoate, the data agree very well with data from other systems. For PEO in indomethacin, the data are closer to the line of unit slope, indicating a stronger coupling between the dynamics of PEO and the host that is consistent with hydrogen bonding. The points for PEO in *o*-terphenyl and toluene fall well below the Lodge−McLeish curve. As discussed in the previous section, for these two systems, the host T_g value does not provide sufficient information to predict blending behavior at the considerably higher temperatures where the NMR measurements are performed.

CONCLUDING REMARKS

We performed NMR measurements on the dynamics of dilute perdeuteriopoly(ethylene oxide) in four low molecular weight glass-formers: sucrose benzoate, indomethacin, *o*-terphenyl, and toluene. The results were compared with literature data on dilute PEO in poly(methyl methacrylate) and poly(vinyl acetate) hosts. We also compared the dilute PEO systems with the literature for other dilute polymer mixtures.

We find that the segmental dynamics of PEO are strongly correlated with the dynamics of the hosts regardless of whether the host is a polymer or a low molecular weight glass-former. For dilute PEO in mixtures with PMMA, PVAc, and sucrose benzoate, the Lodge−McLeish model with a ϕ_{self} of 0.35 gives a good description of the dynamics of PEO. This is similar to the behavior of dilute polyisoprene blends and dilute polystyrene mixtures. In the presence of strong intermolecular hydrogen bonding, the dynamics of dilute PEO is more tightly coupled to the host dynamics, as demonstrated by results for indomethacin as the host matrix.

Upon mixing, the fundamental factor that controls the dynamics of PEO is the segmental dynamics of the blending partner at the measurement temperature rather than the T_g of the blending partner. Our implementation of the Lodge−McLeish model is suitable for the interpretation of measurements far above T_g only if the two pure components have dynamics with comparable temperature dependences above T_g. For dilute PEO in toluene and *o*-terphenyl, this condition is not satisfied. A quantitative understanding of such systems will require a new approach or a more complex implementation of the Lodge−McLeish model.

ACKNOWLEDGMENT

This research was supported by the National Science Foundation through the Divison of Materials Research, Polymer Program (0907607 and 1104770). Measurements were performed at the Instrument Center of the Department of Chemistry, University of Wisconsin—Madison, supported by NSF CHE-9629688. We thank Charles Fry, Monika Ivancic, and Robert Shanks for their support.

REFERENCES

(1) Klein, R. J.; Runt, J. *J. Phys. Chem. B* **2007**, *111* (46), 13188–13193.
(2) Borodin, O.; Smith, G. D. *Macromolecules* **2006**, *39* (4), 1620–1629.
(3) Lutz, T. R.; He, Y. Y.; Ediger, M. D.; Cao, H. H.; Lin, G. X.; Jones, A. A. *Macromolecules* **2003**, *36* (5), 1724–1730.
(4) Cao, H. H.; Lin, G. X.; Jones, A. A. *J. Polym. Sci., Part B: Polym. Phys.* **2004**, *42* (6), 1053–1067.
(5) Cao, H. H.; Lin, G. X.; Jones, A. A. *J. Polym. Sci., Part B: Polym. Phys.* **2005**, *43* (18), 2433–2444.
(6) Farago, B.; Chen, C. X.; Maranas, J. K.; Kamath, S.; Colby, R. H.; Pasquale, A. J.; Long, T. E. *Phys. Rev. E* **2005**, *72*, 3.
(7) Genix, A. C.; Arbe, A.; Alvarez, F.; Colmenero, J.; Willner, L.; Richter, D. *Phys. Rev. E* **2005**, *72*, 3.
(8) Haley, J. C.; Lodge, T. P. *J. Chem. Phys.* **2005**, *122*, 23.
(9) Jin, X.; Zhang, S. H.; Runt, J. *Macromolecules* **2004**, *37* (21), 8110–8115.
(10) Lodge, T. P.; Wood, E. R.; Haley, J. C. *J. Polym. Sci., Part B: Polym. Phys.* **2006**, *44* (4), 756–763.
(11) Ngai, K. L.; Roland, C. M. *Macromolecules* **2004**, *37* (8), 2817–2822.
(12) Niedzwiedz, K.; Wischnewski, A.; Monkenbusch, M.; Richter, D.; Genix, A. C.; Arbe, A.; Colmenero, J.; Strauch, M.; Straube, E. *Phys. Rev. Lett.* **2007**, *98*, 16.
(13) Maranas, J. K. *Curr. Opin. Colloid Interface Sci.* **2007**, *12* (1), 29–42.
(14) Zhao, J.; Zhang, L.; Ediger, M. D. *Macromolecules* **2008**, *41* (21), 8030–8037.
(15) Lodge, T. P.; McLeish, T. C. B. *Macromolecules* **2000**, *33* (14), 5278–5284.
(16) Urakawa, O.; Ujii, T.; Adachi, K. *J. Non-Cryst. Solids* **2006**, *352* (42−49), 5042–5049.
(17) Tyagi, M.; Arbe, A.; Colmenero, J.; Frick, B.; Stewart, J. R. *Macromolecules* **2006**, *39* (8), 3007–3018.
(18) Tyagi, M.; Arbe, A.; Alegria, A.; Colmenero, J.; Frick, B. *Macromolecules* **2007**, *40* (13), 4568–4577.
(19) Savin, D. A.; Larson, A. M.; Lodge, T. P. *J. Polym. Sci., Part B: Polym. Phys.* **2004**, *42* (7), 1155–1163.
(20) Ediger, M. D.; Lutz, T. R.; He, Y. *J. Non-Cryst. Solids* **2006**, *352* (42−49), 4718–4723.
(21) Yu, L. *Adv. Drug Delivery Rev.* **2001**, *48* (1), 27–42.
(22) Wojnarowska, Z.; Adrjanowicz, K.; Wlodarczyk, P.; Kaminska, E.; Kaminski, K.; Grzybowska, K.; Wrzalik, R.; Paluch, M.; Ngai, K. L. *J. Phys. Chem. B* **2009**, *113* (37), 12536–12545.
(23) Andronis, V.; Zografi, G. *Pharm. Res.* **1998**, *15* (6), 835–842.
(24) Andronis, V.; Zografi, G. *Pharm. Res.* **1997**, *14* (4), 410–414.
(25) Wu, T.; Yu, L. *J. Phys. Chem. B* **2006**, *110* (32), 15694–15699.
(26) Liu, W.; Bedrov, D.; Kumar, S. K.; Veytsman, B.; Colby, R. H. *Phys. Rev. Lett.* **2009**, *103*, 3.

(27) Mark, J. E. *Physical Properties of Polymer Handbook*, 2nd ed.; Springer: New York, 2006.
(28) Bovey, F. A. *NMR of Polymers*; Academic Press: San Diego, 1996.
(29) Zhu, W.; Ediger, M. D. *Macromolecules* **1995**, *28* (22), 7549–7557.
(30) He, Y. Y.; Lutz, T. R.; Ediger, M. D.; Ayyagari, C.; Bedrov, D.; Smith, G. D. *Macromolecules* **2004**, *37* (13), 5032–5039.
(31) Bandis, A.; Wen, W. Y.; Jones, E. B.; Kaskan, P.; Zhu, Y.; Jones, A. A.; Inglefield, P. T.; Bendler, J. T. *J. Polym. Sci., Part B: Polym. Phys.* **1994**, *32* (10), 1707–1717.
(32) Min, B. C.; Qiu, X. H.; Ediger, M. D.; Pitsikalis, M.; Hadjichristidis, N. *Macromolecules* **2001**, *34* (13), 4466–4475.
(33) Qiu, X. H.; Moe, N. E.; Ediger, M. D.; Fetters, L. J. *J. Chem. Phys.* **2000**, *113* (7), 2918–2926.
(34) Lutz, T. R.; He, Y. Y.; Ediger, M. D. *Macromolecules* **2005**, *38* (23), 9826–9835.
(35) He, Y. Y.; Lutz, T. R.; Ediger, M. D. *J. Chem. Phys.* **2003**, *119* (18), 9956–9965.
(36) Lutz, T. R.; He, Y. Y.; Ediger, M. D.; Pitsikalis, M.; Hadjichristidis, N. *Macromolecules* **2004**, *37* (17), 6440–6448.
(37) Jin, X.; Zhang, S. H.; Runt, J. *Macromolecules* **2003**, *36* (21), 8033–8039.
(38) Zhang, S. H.; Painter, P. C.; Runt, J. *Macromolecules* **2002**, *35* (25), 9403–9413.
(39) Zhang, S. H.; Painter, P. C.; Runt, J. *Macromolecules* **2002**, *35* (22), 8478–8487.
(40) Greet, R. J.; Turnbull, D. *J. Chem. Phys.* **1967**, *46* (4), 1243.
(41) Richert, R. *J. Chem. Phys.* **2005**, *123*, 15.
(42) Santos, F. J. V.; de Castro, C. A. N.; Dymond, J. H.; Dalaouti, N. K.; Assael, M. J.; Nagashima, A. *J. Phys. Chem. Ref. Data* **2006**, *35* (1), 1–8.
(43) Hinze, G.; Sillescu, H. *J. Chem. Phys.* **1996**, *104* (1), 314–319.
(44) Rossler, E.; Sillescu, H. *Chem. Phys. Lett.* **1984**, *112* (1), 94–98.
(45) Dries, T.; Fujara, F.; Kiebel, M.; Rossler, E.; Sillescu, H. *J. Chem. Phys.* **1988**, *88* (4), 2139–2147.
(46) Cangialosi, D.; Schwartz, G. A.; Alegria, A.; Colmenero, J. *J. Chem. Phys.* **2005**, *123*, 14.
(47) Adam, G.; Gibbs, J. H. *J. Chem. Phys.* **1965**, *43* (1), 139.
(48) Cangialosi, D.; Alegria, A.; Colmenero, J. *Macromolecules* **2006**, *39* (20), 7149–7156.
(49) Kamath, S.; Colby, R. H.; Kumar, S. K.; Karatasos, K.; Floudas, G.; Fytas, G.; Roovers, J. E. L. *J. Chem. Phys.* **1999**, *111* (13), 6121–6128.